Advances on Polarization Modulator Technology and Methodology for Future Improvements

G. Savini [1*], J.Zhang [2], P.Ade [2], P.D.Mauskopf [2]
[1] Optical Science Laboratory, University College London, Gower Street, London, WC1E 6BT, U.K.
[2] School of Physics and Astronomy, Cardiff University, Queens Buildings, the Parade, Cardiff, CF24 3AA, U.K
[*1] Email: gs@star.ucl.ac.uk

Abstract: In this work we present the latest improvements on the fabrication of a non-crystal achromatic half-wave plate working in the sub-THz frequency range [1]. This is achieved by hot-pressing polypropylene layers with photo-lithographed copper structures. We will discuss the performance of the first prototypes and a few techniques for the improvement of future designs. General considerations at the root of achromatic designs will also be touched upon which are valid for both optical and waveguide phase modulators.

Keywords: Polarization modulator technology, Non-crystal achromatic half-wave plate, Sub-THz

doi: 10.11906/TST.109-115.2011.09.16

1. Introduction

Half-wave plates in the mm-wavelength region are of use in a range of different physical experiments. Each application dictates specific requirements for the device adopted. In astronomy, one of the main characteristics due to photon-starved experiments is the broad-band nature of the phase modulator. Most experiments employ 3 or more contiguous spectral bands each with a relative bandwidth $2(\nu_{max}-\nu_{min})/(\nu_{max}+\nu_{min})$ of ~ 0.3. The result is the requirement for a very a-chromatic phase modulator for each band and even more so if the modulator is employed across more than one band. Previous designs [2,3,4] have used a set of crystal birefringent discs arranged in a given configuration [5] to produce a quasi-flat phase shift across a large range of frequencies. These have been characterized thoroughly [3,4] and have shown good performances both warm and cold.

Limitations in their use at frequencies higher than a few hundred GHz due to the absorption characteristics of sapphire require the plate to be always cooled to low temperatures (<100*K*) so to substantially decrease the absorption of the crystal with practical implications for the experiment design and a non-100% survival rate of the necessary anti-reflection coating for such a high impedance miss-match (return-loss). The adoption of the photolithographic technique on polypropylene substrates (already employed on frequency selecting filters [8]) which has a good track record of cryogenic environment operation was successful in producing a combination of inductive and capacitive grids [9] to produce a first prototype of an air-gap metal-mesh half-wave plate [10]. The performance of this latter device reported in [10] is equivalent (in terms of a-chromatic phase flatness) to that of a 3-plate stack according to published configurations based on [5] and [7], but with substantial less absorption loss and emissivity. The subsequent step was the simulation via lumped element Transmission-Line and Finite Element Analysis package HFSS [11] of a compact design where polypropylene layers replaced the air-gaps and

modifications made to the grid geometry to compensate for the extended bandwidth attempted in the prototype design. We describe here the main features of these prototypes and make some general considerations of employability while the detailed results of the design study and prototype of a "hot-pressed metal-mesh waveplate" (hereafter HPWP) are reported in [1].

2. MAIN RESULTS

The first prototype was designed for an 80% bandwidth (3.5 to 9.5 cm^{-1}), and the parametric TL design of capacitive and inductive grids was limited to a few parameters for ease of study convergence and fabrication. Unlike the air-gap prototype in [10], the hot-pressed version presents a substrate Fabry-Perot fringe (fig.2) due to the thickness of the overall substrate that can be altered to some extent but not removed completely without applying an anti-reflection coating. As reported in [1], the device which can be improved with further parametrization of the layer spacing provides a modulation efficiency of 85% in a 90% spectral bandwidth and a maximum of 96% modulation efficiency in two narrow bands centred at 125 and 295 *GHz*.

The full design of the prototype is included in Table 1 of [1] and is comprised of a set of 12 metal-mesh layers (6 inductive and 6 capacitive) embedded in a total thickness of ~3*mm* of polypropylene. This allows the HPWP to be easy to handle with a very low risk of damaging the object or changing its properties. In addition, filters with identical materials and manufacturing procedure have already been successfully flown on satellites guaranteeing an off-the-shelf Technology Readiness Level rating to these devices.

（a） (b)

Fig. 1 A 97*GHz* 40% bandwidth prototype HPWP in (a) ambient and (b) reflected illumination. The nature of the object allows for easy handling and low environment degradation.

Further improvement on the transmission of the prototype (which can be seen in Fig.2) can be obtained by bonding a layer of porous PTFE (with a level of porosity to achieve an effective dielectric constant of ~1.5).

The performance of the HPWP was measured (as described in [1]) with a polarized spectrometer, and the results are reported below.

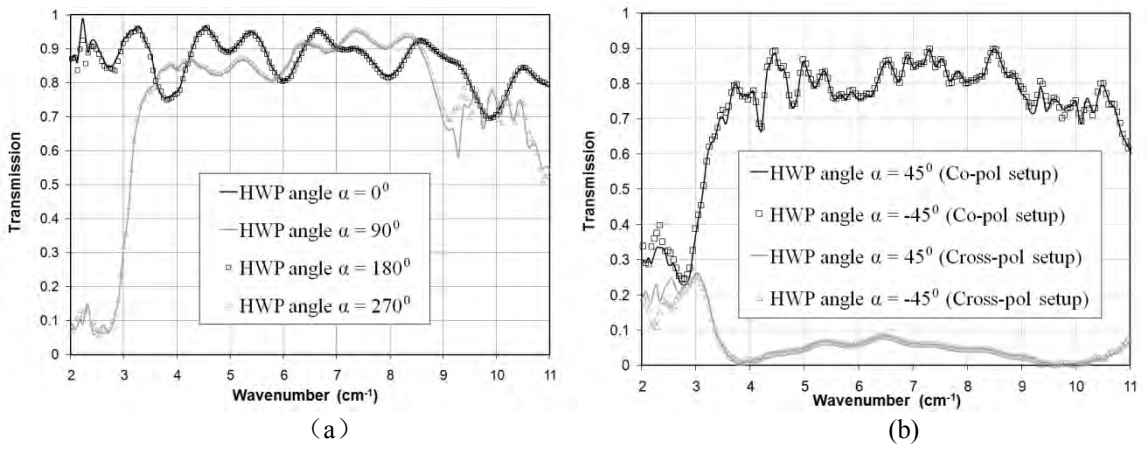

Fig. 2 Transmission at various angles of incident polarization of the HPWP. (a) On axis transmissions between aligned polarizers. (b) Transmissions at 45 deg wrt crossed polarizers denoting the polarization rotation action of the device. Symbols and solid lines are transmissions at 180 degrees difference taken subsequently (where no change is expected) to emphasize the stability of the measurement system.

3. ACHROMATIC COMBINATION

The phase of the final prototype was not as flat (or close to 180°) as was predicted by the model (fig. 13 in [1]). The main reason for this is expected to be the non-appropriate skin depth of the copper deposition together with the possible slight mis-alignment of the grids with respect to the modeled configuration (fig.5 of [1]).

While a second prototype is in study by allowing inter-mesh thickness to vary separately hence increasing the number of parameters, we considered the possibility of adopting a technique adopted in the crystal plates to expand the range of frequencies where the phase-shift is effective.

We attempted to adopt the same Pancharatnam conditions (below) used to combine linear phase-shift crystal plates as in [2], [3] and [4] but to apply them to our prototype device with its measured phase-shift function. The technique adopted by Pancharatnam is to impose a set of rotations (equivalent to phase shifts) by $[2\delta_i - \alpha, 2\delta_i, 2\delta_i + \alpha]$ degrees around axes corresponding to a given orientation of a phase shifting element, respectively for the same polarization state at different spectral frequencies (denoting by "$2\delta_i$" the frequency dependant phase shift of the i-th element of a stack). Imposing that these 3 frequencies subject to a difference in phase shift are to be shifted by ultimately the same amount (Δ) after all such rotations, the values for the single phase shifts "$2\delta_i$" and that of the angles "c_i" between the fast axis of the first and second element are obtained.

In our case, the "$2\delta_i$" frequency dependant phase shift of the i-th element of a stack is the thin smooth function in the left plot of fig.4, "2Δ" the phase shift of the stack-equivalent plate and "γ" the angle between the fast angle of the equivalent stack and that of the first element.

We can re-write the two fundamental conditions in [5] as:

$$\cos\Delta = \cos 2\delta_1 \cos\delta_2 - \sin 2\delta_1 \sin\delta_2 \cos 2c \quad (1)$$

$$\tan 2\gamma = \sin 2c \left(\frac{\sin 2\delta_1}{\tan 2\delta_2} + \cos 2\delta_1 \cos 2c \right)^{-1} \quad (2)$$

Pancharatnam conditions are imposed on a given phase difference (even though the author in [5] associates a 1-to-1 correspondence between wavelength (or frequency) bandwidth and phase shift due to the linearity of crystal phase-shift in this respect).

We apply (1) and (2) imposing $\Delta = 180^\circ$ (we desire a Half-wave plate), while adopting the same element and hence in the case that $\delta_1 = \delta_2$. But differently from the choice of a crystal thickness in [5] we select a value of δ_1 which is at the center of the range of variation of the phase shift (roughly equal to 80 degrees as $2\delta_1$ relates to the phase shift of the device). And request that the same conditions in (1) and (2) be verified for this value of δ_1 and for values differing from δ_1 by $\pm\alpha$. The value of α being chosen to extend to the limit the band in which the device will perform achromatically.

The transcendental nature of the equation does not allow for an exact analytical solution so numerical solutions are obtained and in fact it is easy to produce a full phase-space of solutions to check how close to a solution is a given value of phase shift.

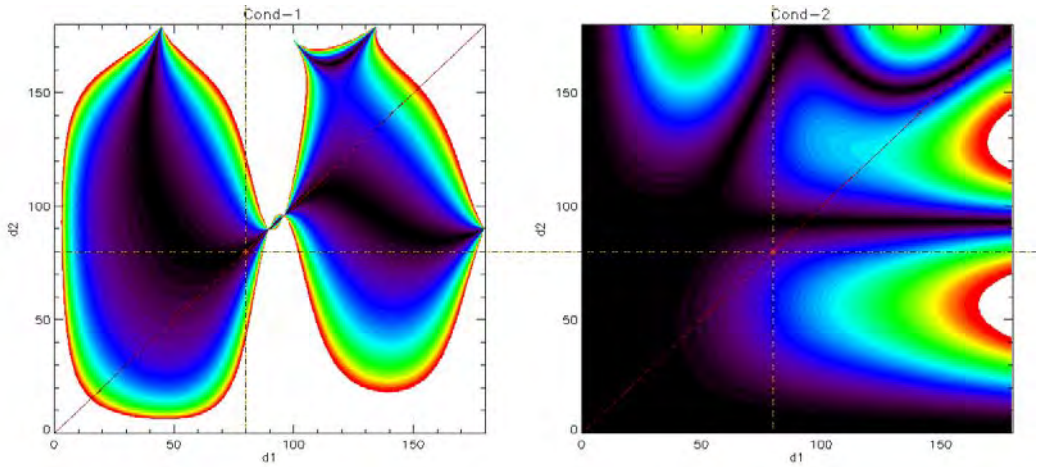

（a） (b)

Fig. 3 (a) A contour plot where the value of the residual from imposing equation (1) on 3 values of phase shift is shown (black=0 residual indicates the region where the best values of $\boldsymbol{\delta_1}$ and $\boldsymbol{\delta_2}$ are found. (b) The equivalent for condition (2). While it is in general possible to adopt elements (or plates) with different phase shift, in this particular case, as we are combining the same element, only the diagonal of the plots is being considered. A vertical and horizontal line is shown on both plots to indicate the imposed center value of the half-phase shift (80 degrees). This can be seen to be optimal in the left plot and quasi-optimal in the right plot.

Having imposed Δ and chosen the values for δ_1, δ_2 from (1), we recover the angle "c" at which it is necessary to rotate the intermediate (or central) element in order to achieve the closest phase shift (between two designated equivalent axis) to "2Δ". This is illustrated in fig.4 (a) where

contour levels of c-values are shown in correspondence with the chosen values as mentioned above. The intersection of the lines identifies an angle of roughly 57.5 degrees.

The stack we are in search of will then contain three identical elements with their primary[i] axis at the angles (0-57.5-0). At these angles the residual from the numerical solution of these equations assumes a minimum. This 3-element achromatic device will also have an equivalent axis which is identified as the additional value of "c" is chosen by solving (2) for "γ" as is given from a contour in fig.4 (b). This angle is referenced to the same primary axis of the first and last element of the stack.

It is worth noting that this is only an "effective" axis in as much that it is averaged over the frequency band where the phase shift condition is imposed.

From what has been discussed it is a direct conclusion that the parameters of the stack are a complex function of the phase shift of the single element at the frequencies of interest. Different frequencies at which a different phase shift is produced would in turn require slightly different angles in both "c" and "γ" values. The immediate consequence of this is that the recovered "effective" axis is defined by the frequency band but more importantly by the spectral nature of the source observed. This was conclusion was also drawn for a crystal stack of plate in [4] where detailed spectroscopic analysis shows a small frequency variation of such orientation.

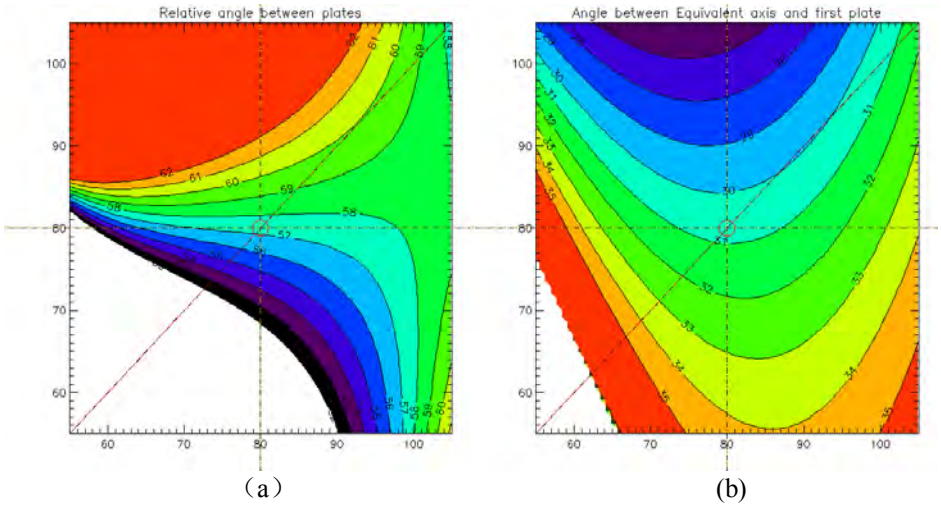

Fig. 4 (a) Contour levels of the value of "c", the angle between the same primary axis of the first and last stack element with the intermediate one. (b) Contour plot of the values of the "effective" primary axis of the constructed stack. Both: chosen values for the phase shift are indicated by the orthogonal crossing lines. Both plots are for a Δ of 90 degrees. The right plot is also dependent on the fixed value of 57.5 degrees for "c" suggested by the left plot.

The resulting phase of a stack of 3 of these prototypes (fast axis at 0-57-0 respectively) is modeled with a simple Jones matrix cascade by using a smoothed version of the phase shift of the single element (Fig.5 (a)). The recovered stack phase is very flat comparing to that of the single device (Fig.5). This is attributed to the slower variation with wavelength of the actual phase function of the device (with respect to the linear variation of a birefringent crystal). This

approach is purely a mathematical result of a set of rotations on the Poincare' sphere (illustrated in [6]), as such it is decoupled from the technological case in question. The same technique was in fact also successfully adopted in a waveguide component [12] in order to obtain an exceedingly flat phase in a 40% bandwidth.

It should be noted that while the ideal phase resulting is optimal, the combination of 3 of the built prototypes with their inherent impedance mismatch (or non unit transmission in fig.2) makes such a device less attractive. The important result in this phase manipulation is to allow to "relax" the phase condition of a flat 180-degree shift in the parametric modeling of the prototype. The available parameters of geometry and spacing can then be varied to obtain the best possible impedance match with free space while allowing multiple-element combination to improve on the phase flatness.

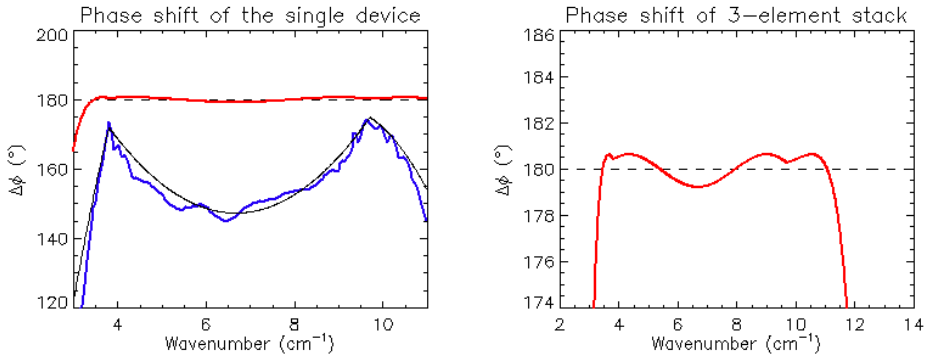

Fig. 5 (a) Recovered phase measured from the HPWP prototype with overlay of the smooth function used to simulate the stack phase (Jones formalism). (b) Closer y-axis range of the stack phase of 3-elements

References

[1] J. Zhang, P.A.R. Ade, P.D. Mauskopf, G. Savini, L.Moncelsi, N.Whitehouse, "Polypropilene embedded metal mesh broadband achromatic half-wave plate for millimetre wavelengths" , *Appl. Opt.* 50, 3750–3757 (2011).

[2] A. M. Title and W. J. Rosenberg, "Achromatic retardation plates", *Proc. SPIE* 307, 120–131 (1981).

[3] G. Pisano, G. Savini, and P. A. R. Ade, "Achromatic half-wave plate for submillimeter instruments in cosmic microwave background astronomy: experimental characterization", *Appl. Opt.* 45, 6982–6989 (2006).

[4] G. Savini, P.A.R.Ade, J.House, G.Pisano, V.Haynes, P.Bastien, "Recovering the frequency dependent modulation function of the achromatic half-wave plate for POL-2: the SCUBA-2 polarimeter", *Appl. Opt.* 48, 2006–2013 (2009).

[5] S. Pancharatnam, "Achromatic combinations of birefringent plates", *Raman Research Institute, Bangalore, Memoir* 71, 137–144 (1955).

[6] G. Savini, G. Pisano, and P. A. R. Ade, "Achromatic half-wave plate for submillimeter instruments in cosmic microwave background astronomy: modeling and simulation", *Appl. Opt.* 45, 8907–8915 (2006).

[7] T. Matsumura, S. Hanany, P. A. R. Ade, B. R. Johnson, T. J.Jones, P. Jonnalagadda, and G. Savini, "Performance of three- and five-stack achromatic half-wave plates at millimetre wavelengths", *Appl. Opt*. 48, 3614–3625 (2009).

[8] P. Ade, G. Pisano, C. Tucker, and S. Weaver, "A review of metal mesh filters", *Proc. SPIE* 6275, (2006).

[9] A.D.Shatrow,A.D.Chuprin, andA.N.Sivov, "Constructing the phase converters consisting of arbitrary number of translucent surfaces", *IEEE Trans. Antennas Propag.* 43, 109–113 (1995).

[10] G. Pisano, G. Savini, P. A. R. Ade, and V. Haynes, "Metal-mesh achromatic half-wave plate for use at submillimeter wavelengths", *Appl. Opt*. 47, 6251–6256 (2008).

[11] AnsoftHFSSwebsite: http://www.ansoft.com/products/hf/hfss /.

[12] G. Pisano, S.Melhuish, G. Savini, L.Piccirillo, B.Maffei, "A broadband W-band Polarization rotator with very low cross polarization", *IEEE Microwave and Wireless Components Letters* 21, 127-129 (2011).

[i] For primary axis we suggest that as the object is symmetrical an equivalent nomenclature as that adopted in the case of bi-refringent crystals (fast/slow, ordinary/extra-ordinary, primary/secondary) be adopted. With such a definition a rotation of an element of a stack with respect to another can be likened to the rotation of a given axis.